

FATIGUE MODEL FOR FIBER-REINFORCED POLYMERIC COMPOSITES

by

Hai C. Tang, Tinh Nguyen,
Tze-jeer Chuang, Joannie Chin and H. Felix Wu
National Institute of Standards and Technology
Gaithersburg, MD 20899 USA
and
Jack Lesko
Virginia Polytechnic Institute and State University
Blacksburg, VA 24061

Reprinted from the *Journal of Materials in Civil Engineering*, Vol. 12, No. 2, 97-104, May 2000.

NOTE: This paper is a contribution of the National Institute of Standards and Technology and is not subject to copyright.



NIST

National Institute of Standards and Technology
Technology Administration, U.S. Department of Commerce

FATIGUE MODEL FOR FIBER-REINFORCED POLYMERIC COMPOSITES

By Hai C. Tang,¹ Member, ASCE, Tinh Nguyen,² Tze-jeer Chuang,³ Joannie Chin,⁴ Jack Lesko,⁵ and H. Felix Wu⁶

ABSTRACT: A fatigue model based on cumulative damage is developed for predicting the fatigue life of fiber-reinforced polymeric composites. This model incorporates applied maximum stress, stress amplitude, loading frequency, residual tensile modulus, and material constants as parameters. The model is verified with experimental fatigue data on a glass fiber/vinyl ester composite. While the specimens are exposed to air, freshwater, or seawater at 30°C, they are subjected to tension-tension stress at four levels of applied maximum tensile stress in each of two frequencies. Both the residual mechanical properties at specified loading cycles and the number of cycles at which the specimens fail are measured. The results show that, for the material used in this study, the loss in residual tensile strength and modulus in saltwater is approximately the same as that in freshwater and that the fatigue life in these aqueous environments is shorter than that in air. Numerical analysis is carried out to determine the material constants of the composite. The fatigue model agrees well with the experimental data. The model can be used to predict the fatigue life of the polymeric composites subjected to an applied load in different environments and to predict the residual tensile modulus after a number of cycles of service at a given load.

INTRODUCTION

Over the last three decades, fiber-reinforced polymeric composites have been extensively used in a wide range of aerospace and military applications. There is a growing interest in extending the use of these materials into civil engineering applications, including offshore structures (Wang and Fitting 1995; Saadatmanesh and Ehsani 1998). There is an urgent need to develop quantitative analysis and methodology for assessing the safety and reliability of using polymeric composites in these applications. One particularly critical issue in regard to using polymeric composites in structural applications is their fatigue reliability in different environmental and loading conditions. Fatigue damages in polymeric composites for noncivil engineering applications have been extensively investigated (Reifsnider 1979, 1991; Talreja 1987; Jang 1994; Martin 1995). Studies of the effects of water or saltwater on the fatigue behavior of polymeric composites have been reported (Watanabe 1979; Springer et al. 1980; Hofer et al. 1987; Komai et al. 1991; Chiou and Bradley 1996; Adimi et al. 1998). However, there is little quantitative research on the effects of civil engineering environments, namely, water, seawater, concrete pore solution, temperature, ultraviolet light, and loading on the fatigue of polymeric composites. The main objective of this study is to develop experimentally verifiable models for predicting the fatigue life of polymeric composites.

This paper presents the development and experimental verification of a fatigue model for a vinyl ester/E-glass fiber composite subjected to tension-tension loading at four levels of

maximum applied stress in each of two frequencies in air, freshwater, and saltwater environments. The model can be used to predict the fatigue life of polymeric composites under an applied load and to estimate the residual tensile modulus after a certain number of loading cycles.

DERIVATION OF FATIGUE MODEL

The basic failure mechanisms of polymer composites subjected to tension-tension fatigue are matrix cracking, interface debonding, delamination, splitting, and fiber breakage (Talreja 1987; Ye 1989; Plumtree and Shen 1991; Ashbee 1993; Jang 1994; Reifsnider 1994). The cumulative damage as a function of the number of loading cycles may be generally described by the curve in Fig. 1. Matrix cracks, the first to occur in the fatigue process, are due to a high concentration of stress. As the number of cracks increases, stress redistribution reduces the initiation of new cracks, and damage appears to grow at a constant rate as cyclic loading continues. In the region of damage, interfacial bonding, delamination, and fiber breaking start to occur and gradually increase. Fiber breakage increases due to the continuing growth of matrix cracks and fiber-matrix debonding. As the breakage progresses and intensifies, the rate of fiber fracture increases rapidly and, finally, the composite ruptures.

The change of modulus has been commonly used to express the state of damage in polymer composites (Ye 1989; Plumtree

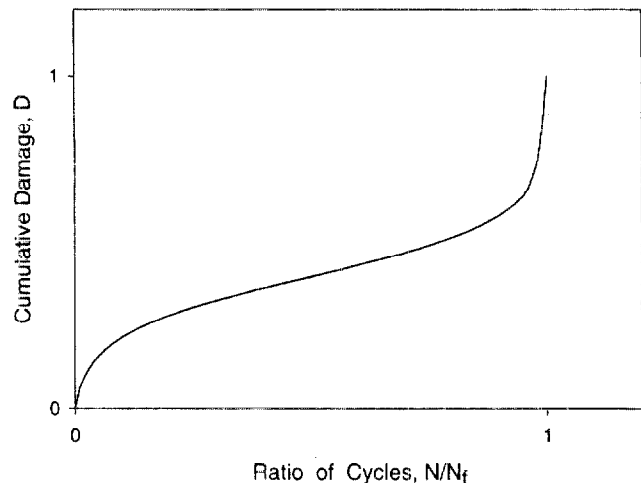


FIG. 1. Cumulative Damage as Function of Number of Cycles

¹Comp. Specialist, High Perf. Sys. and Services Div., Information Technol. Lab., Nat. Inst. of Standards and Technol., Gaithersburg, MD 20899-8951.

²Phys. Sci., Build. Mat. Div., Build. and Fire Res. Lab., Nat. Inst. of Standards and Technol., Gaithersburg, MD 20899-8621.

³Physicist, Ceramics Div., Mat. Sci. and Engrg. Lab., Nat. Inst. of Standards and Technol., Gaithersburg, MD 20899-8521.

⁴Mat. Res. Engr., Build. Mat. Div., Build. and Fire Res. Lab., Nat. Inst. of Standards and Technol., Gaithersburg, MD.

⁵Asst. Prof., Engrg. Sci. and Mech. Dept., Virginia Polytechnic Inst. and State Univ., Blacksburg, VA 24061-0219.

⁶Program Mgr. for Compos. Mat., Advanced Technol. Program, Nat. Inst. of Standards and Technol., Gaithersburg, MD 20899-4730.

Note. Associate Editor: Christopher K. Y. Leung. Discussion open until October 1, 2000. To extend the closing date one month, a written request must be filed with the ASCE Manager of Journals. The manuscript for this paper was submitted for review and possible publication on May 26, 1998. This paper is part of the *Journal of Materials in Civil Engineering*, Vol. 12, No. 2, May, 2000. ©ASCE, ISSN 0899-1561/00/0002-0097-0104/\$8.00 + \$.50 per page. Paper No. 18450.

and Shen 1991; Subramanian et al. 1995). In this work, cumulative damage D is defined

$$D = 1 - \frac{E}{E_0}$$

where E and E_0 = residual and initial moduli, respectively.

Thionnet and Renard (1994) described the growth of damage of laminated composites under fatigue loading as a function of damage D and a set of parameters that characterize the mechanical environments such as the minimum/maximum stress ratio, the frequency, and the temperature. They further separated the function as a product of a function of the damage and a function of mechanical environments

$$\frac{dD}{dN} = f(D, p(N)) = f_1(D)f_2(p(N))$$

where $p(N)$ = parameter describing the mechanical environments.

In a similar way we define the incremental damage per loading cycle as a function of cumulative damage D and a constant that may be dependent on the minimum/maximum stress ratio, the frequency, the temperature, and exposure media such as humidity, water, and saltwater. This function may be derived from the general plot of the cumulative damage versus the number of fatigue cycles as shown in Fig. 1 (Ye 1989; Plumtree and Shen 1991). The derivative of the function rapidly decreases at the beginning, maintains at a constant as fatigue loading continues, and then rapidly increases near the end of the life cycles, as depicted in Fig. 2. The initial damage growth per loading cycle may be mathematically expressed in either of the following two functions:

$$\frac{dD}{dN} = \frac{C_1}{D^{n_1}}$$

or

$$\frac{dD}{dN} = C_1 e^{-n_1 D}$$

where N = number of loading cycles; and C_1 and n_1 = constants; and $n_1 > 1$. Thus, the damage growth near the end of the life cycle before failure may be described

$$\frac{dD}{dN} = \frac{C_2}{(1-D)^{n_2}}$$

or

$$\frac{dD}{dN} = C_2 e^{n_2 D}$$

where C_2 and n_2 = constants, and $n_2 > 1$.

The general fatigue model as depicted in Fig. 2 may take the form

$$\frac{dD}{dN} = \frac{C_1}{D^{n_1}} + \frac{C_2}{(1-D)^{n_2}} \quad (1)$$

or

$$\frac{dD}{dN} = C_1 e^{-n_1 D} + C_2 e^{n_2 D} \quad (2)$$

However, our experimental data on the cumulative damage D , as a function of the number of loading cycles N , for the vinyl ester/E-glass fiber composite used in this study do not show any initial weakening of material strength until the number of loading cycles exceeds 1,000 (Fig. 3). Further, data on initial damage do not reveal any evidence of an abrupt growth phenomenon. Instead, the data show smooth, gradual increases

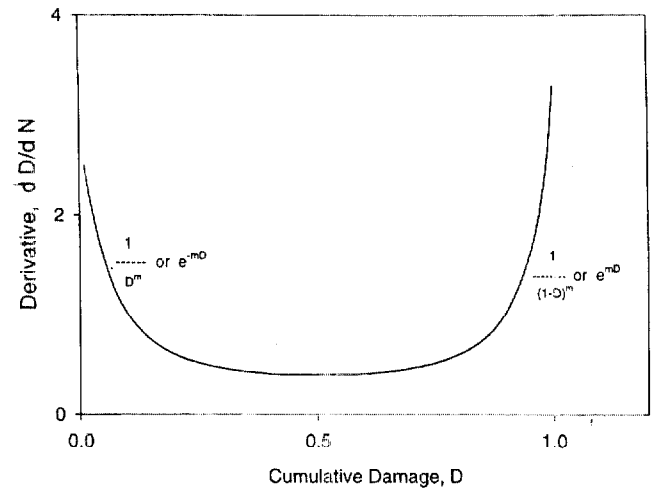


FIG. 2. Damage Growth per Cycle

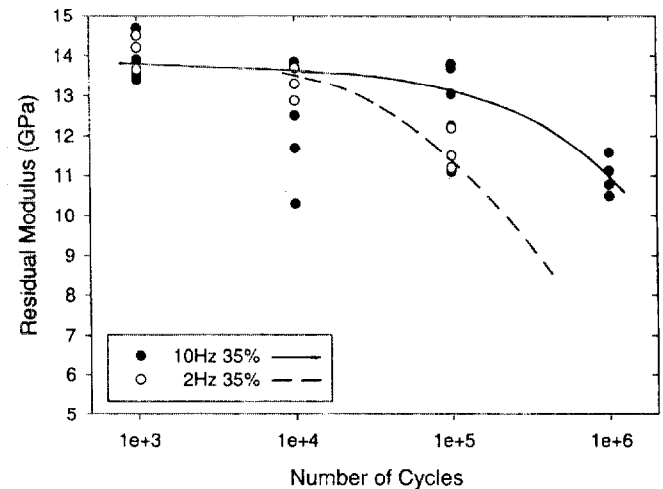


FIG. 3. Residual Modulus at 2 and 10 Hz and 35% Ultimate Load

from zero damage. This observation is similar to that reported previously for an unidirectional glass fiber/epoxy composite, which showed little degradation in modulus due to fatigue in laminae until the end of the life cycle (Kadi and Ellyin 1994). Therefore, for the composite material used in this study, C_1 is negligible in comparison with C_2 . Consequently, the damage rate per loading cycle may be expressed by

$$\frac{dD}{dN} = \frac{C}{(1-D)^n} \quad (3)$$

or

$$\frac{dD}{dN} = C e^{nD} \quad (4)$$

In the above two equations, the C values may be different, but they merely represent different scale factors to the growth of damage (dD/dN). To determine which of the above two equations is more suitable to describe the fatigue damage phenomenon in polymeric composites, we set C equal to 1 and plot the damage curves represented by (3) and (4) for several n values; these results are shown in Fig. 4. From this figure, (3) seems to better represent the sudden rupture of the composite material as D approaches unity. Therefore, (3) will be expanded to describe the fatigue process for the vinyl ester/E-glass fiber composites used in this study.

Besides the state of damage, the maximum stress and stress

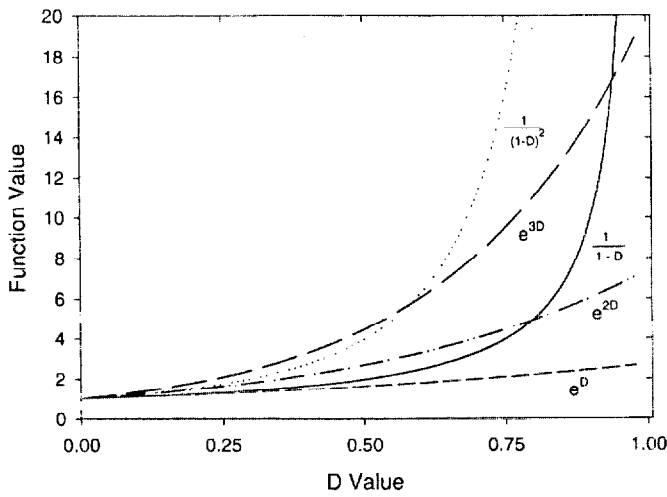


FIG. 4. Comparison between e^{mD} and $1/(1-D)^m$

amplitude may have substantial effects on damage growth (Wnuk 1974a,b; Spearing et al. 1992; Thionnet and Renard 1994). Likewise, temperature T (Ye 1989) and frequency f can also affect the fatigue damage (Wnuk 1974b). Therefore, the C in (3) can be a function of the maximum stress, stress amplitude, temperature, and frequency

$$C = C(\sigma_{\max}, \sigma_{\text{amp}}, T, f)$$

This functional form is similar to those proposed for fatigue of laminated composites (Ogin et al. 1985; Spearing et al. 1992; Liu and Lessard 1994; Thionnet and Renard 1994) and of random short fiber molding composites (Ye 1989). Additionally, Wnuk (1974a,b) has used power form to describe fracture growth in fatigue process in rate sensitive solids. Taken altogether, the C in (3) may be expressed

$$C = \bar{C}(T, f)F(\sigma_{\max}, \sigma_{\text{amp}}) = \bar{C}(T, f)\sigma_{\max}^{m_1}\sigma_{\text{amp}}^{m_2}$$

To make above equation treatable, we further assume $m_1 = m_2 = m$. Accordingly, (3) may be rewritten

$$\frac{dD}{dN} = \bar{C} \frac{(\sigma_{\max}\sigma_{\text{amp}})^m}{(1-D)^n} \quad (5)$$

where \bar{C} , m , and n = material constants; σ_{\max} = maximum stress; σ_{\min} = minimum stress; and σ_{amp} = cyclic stress amplitude, equal to $(\sigma_{\max} - \sigma_{\min})$.

We can express maximum stress and stress amplitude in normalized terms to the ultimate tensile strength σ_{ult} and the minimum to maximum stress ratio R

$$S_{\max} = \frac{\sigma_{\max}}{\sigma_{\text{ult}}}$$

$$S_{\text{amp}} = \frac{\sigma_{\text{amp}}}{\sigma_{\text{ult}}} = \frac{\sigma_{\max} - \sigma_{\min}}{\sigma_{\text{ult}}} = \frac{\sigma_{\max}}{\sigma_{\text{ult}}} \left(1 - \frac{\sigma_{\min}}{\sigma_{\max}}\right) = S_{\max}(1-R)$$

Substituting σ_{\max} and σ_{amp} into (5) and then simplifying, the equation becomes

$$\frac{dD}{dN} = C \frac{(S_{\max}^2(1-R))^m}{(1-D)^n} \quad (6)$$

where $|S_{\max}| \leq 1$ and $C = \bar{C}(\sigma_{\text{ult}})^{2m}$.

Integrating (6) and substituting the initial condition (i.e., $D = 0$ when $N = 0$) we obtain

$$\frac{1}{n+1} - \frac{(1-D)^{n+1}}{n+1} = C(S_{\max}^2(1-R))^m N \quad (7)$$

where $0 \leq D \leq 1$.

When the number of loading cycles approaches the maximum number of life cycles N_f , D approaches 1. Under this condition, (7) becomes

$$\frac{1}{n+1} = C(S_{\max}^2(1-R))^m N_f \quad (8)$$

This formula can also be expressed in log-log form

$$\log \sigma_{\max} = m \log N_f + C \quad (9)$$

In the model validation section, this equation will be shown to fit our experimental data better than commonly used semilog form for fatigue life (Mandell 1982; Mandell and Meier 1983; Ye 1989)

$$\sigma_{\max} = m \log N_f + C \quad (10)$$

DETERMINATION OF MATERIAL CONSTANTS

The constants m , n , and C in (7) and (8) can be obtained from experimental data. This section describes the methodologies of determining these constants.

By taking a logarithm on both sides of (8), we obtain

$$\log[(n+1)C] + 2m \log(S_{\max}) + m \log(1-R) + \log N_f = 0 \quad (11)$$

Therefore, the linear regression slope ($-1/2m$) of the S_{\max} versus N_f plot in log-log scale can be used to compute the material constant m .

To determine the value of n , we need to use the solution at an intermediate state with partial damage D in (7). As evidenced from our experimental data (e.g., Fig. 3), $D(D = 1 - E/E_0)$ is less than 20% up to 10^5 loading cycles for 2 Hz and up to 10^6 cycles for 10 Hz. Therefore, D is relatively small until it approaches the maximum number of life cycles. We can expand the $(1-D)^{n+1}$ term with Taylor's series and omit higher order terms. Accordingly, (7) becomes

$$\begin{aligned} \frac{1}{n+1} \left(1 - 1 + (n+1)D - \frac{(n+1)n}{2!} D^2 + \dots\right) \\ = C(S_{\max}^2(1-R))^m N \end{aligned} \quad (12)$$

For the same applied load where residual moduli are measured at two different numbers of cycles N_1 and N_2 , the respective damages D_1 and D_2 can be derived from (12) as follows:

$$D_1 \left(1 - \frac{n}{2} D_1\right) = C(S_{\max}^2(1-R))^m N_1 \quad (13)$$

$$D_2 \left(1 - \frac{n}{2} D_2\right) = C(S_{\max}^2(1-R))^m N_2 \quad (14)$$

Dividing (13) by (14) and canceling the common terms, we have

$$\frac{D_1 \left(1 - \frac{n}{2} D_1\right)}{D_2 \left(1 - \frac{n}{2} D_2\right)} = \frac{N_1}{N_2} \quad (15)$$

or

$$\left(1 - \frac{n}{2} D_1\right) = \frac{N_1 D_2}{N_2 D_1} \left(1 - \frac{n}{2} D_2\right) = K_{12} \left(1 - \frac{n}{2} D_2\right) \quad (16)$$

where

$$K_{12} = \frac{N_1 D_2}{N_2 D_1} \quad (17)$$

Therefore

$$n = \frac{2(1 - K_{12})}{(D_1 - D_2 K_{12})} \quad (18)$$

The remaining parameter C can then be determined using the plot of maximum stress versus the number of cycles at failure ($S-N$ curve) in (8) and the already known m and n values.

It should be noted that material constants C , m , and n could be dependent on the frequency. However, as will be shown in the following section, our experimental data on two frequencies, 2 and 10 Hz, for the composite used in this study indicate that frequency has little effect on m or n , but it has a substantial effect on C .

EXPERIMENTAL PROCEDURE

The material used in these experiments is a pultruded vinyl ester/E-glass fiber composite. The vinyl ester matrix is a commercial product, which cures via a heat-activated free radical mechanism. The composite is fabricated with longitudinal roving and continuous strand mats. Total content of fiber is approximately 45% by mass and 36–37% by volume, of which approximately one-third is the longitudinal fiber. This composite is a similar material to that used in the construction of the Tom's Creek bridge in Blacksburg, Va., in July, 1997. The specimens were cut from the pultruded plate having dimensions of 1,219-mm (48-in.) wide, 457-mm (18-in.) long, and 3.2-mm (1/8-in.) thick along the longitudinal fiber direction to 229-mm (9-in.) long, 25-mm (1-in.) wide, and 3.2-mm (1/8-in.) thick. The edges of the specimens are then coated with epoxy resin to minimize the absorption of water into the composite from the edges. The specimens were untabbed but were wrapped with wires at both ends to improve the gripping.

Fatigue experiments are conducted in a tension-tension mode in the unidirectional fiber direction with an R (minimum stress to maximum stress ratio) value of 0.1. Maximum loads applied range from 35 to 65% of ultimate tensile strength, and frequencies are set at 2 and 10 Hz. The selection of load levels is based on our preliminary study, which showed that these levels were appropriate to obtain meaningful results within a reasonable time. The 2 Hz frequency is used to minimize the generation of heat in the composite during testing, while the 10 Hz is employed to study the effect of frequency. All experiments are conducted at 30°C on a servohydraulic fatigue test frame that has a tension-compression load capacity of 100 kN. The 30°C is employed for ease of control near ambient condition. The specimens were immersed in charcoal filtered tap water where chlorine and minerals were removed and in a 3.5% NaCl solution to simulate freshwater and seawater environments at 65°C for 506 and 451 h, respectively, to reach 95% of saturation. It is noted that seawater is a complex mixture of many chemical compounds (Garrels and Thompson 1962). However, for the purpose of providing a reproducible exposure environment, a 3.5% NaCl (a typical NaCl concentration in seawater) is used for this study. Before fatigue loading, the ultimate tensile strength, modulus and Poisson's ratio are measured in dry air (45% relative humidity at 30°C), freshwater, and seawater environments.

MODEL VERIFICATION

Table 1 summarizes the static mechanical properties of the composite used in this study. This table shows a 25 and 32% reduction of ultimate strength in freshwater and saltwater conditions, respectively, as compared to the dry air environment. And there are 15 and 11% reductions in tensile modulus, respectively. It is noted that statistical bounds of these properties between freshwater and saltwater environments overlap each other. Therefore, the difference of mechanical properties between them is not statistically significant.

Two sets of fatigue experiments are carried out. In the first set, the experiment is stopped at selected numbers of cycles; the specimens are then removed from the testing machine and the residual tensile strength, tensile modulus, and Poisson's ratio are measured. These results provide the partial damages that occur at given numbers of loading cycles. These damages are used to determine the material constant n in (18). In the

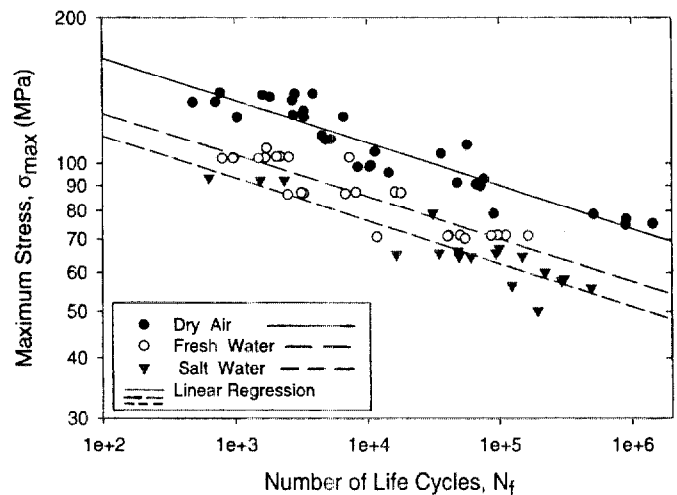


FIG. 5. Fatigue at 10 Hz in Dry Air, Freshwater, and Saltwater

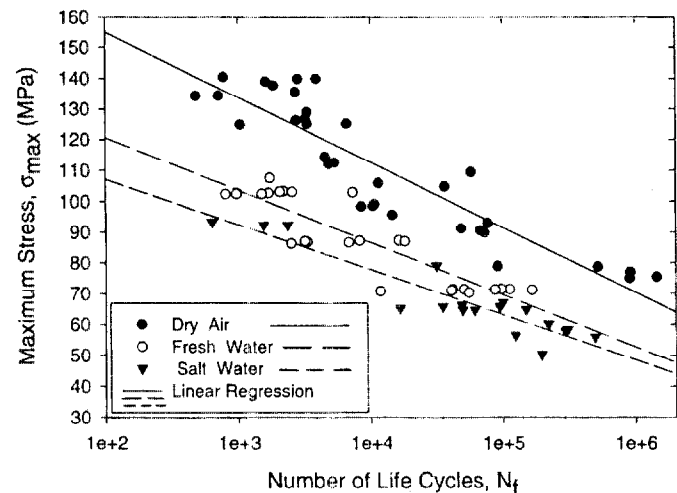


FIG. 6. Fatigue at 10 Hz in Dry Air, Freshwater, and Saltwater

TABLE 1. Mechanical Properties of E-glass/Vinyl Ester Composite

Parameters (1)	Dry Air		Freshwater		Saltwater	
	Mean (2)	Standard deviation (3)	Mean (4)	Standard deviation (5)	Mean (6)	Standard deviation (7)
Ultimate tensile strength (MPa)	212	17.9	158	13.4	144	14.4
Modulus (GPa)	15.55	0.66	13.26	1.20	13.85	4.01
Poisson's ratio	0.31	0.03	0.31	0.03	0.32	0.04

second set, the fatigue experiments are carried out at selected maximum loads until the specimens fail. The applied load and the number of cycles at failure are recorded. These data are used to establish the $S-N$ curves and to verify the fatigue model [(8)]. The data are also employed to determine the value of m in (11).

In Fig. 5, the maximum stress is plotted against the number of cycles at failure in log-log scale for three sets of fatigue experimental data at 10 Hz and 30°C in dry air (45% relative humidity), freshwater, and saltwater environments. In this figure, the symbols represent experimental data and the $S-N$ curves are obtained from the linear regression of the data. The square of linear correlation coefficient (r^2) (Bevington and Robinson 1992) quantitatively indicates the linear correspondence between the maximum stress and the number of cycles at failure. An r^2 value of 1.0 means a perfect linear relationship between the two quantities; a value <1.0 means a less fit. The r^2 values are found to be 0.856, 0.803, and 0.840 for dry air, freshwater, and saltwater, respectively. The same fatigue data are also plotted in semilog scale [i.e., (10)] as shown in Fig. 6. The r^2 for dry air, freshwater, and saltwater environments are 0.824, 0.794, and 0.863, respectively. Based on these r^2 values there is no clear advantage in choosing either formula. However, when we included data at 30% load level in a dry air environment that fail at higher order of cycles, the r^2 for (9) is higher; that is, $r^2 = 0.896$ for (9) versus 0.856 for (10). Therefore, we select (9) to describe the fatigue of the polymeric composite used in this study.

The experimental data show that there is a strong linear relationship between $\log(\sigma_{\max})$ and $\log(N)$ substantiating the validity of the fatigue model. It is interesting to note that there is little difference in the slopes of the linear-regressed lines for the three environments, suggesting that the failure mechanism is probably similar for all three environments. Fig. 5 also reveals that, under the same applied load, the fatigue life of the composite in air is greater than that in freshwater or saltwater and that the difference in fatigue lives between freshwater and saltwater environments is small.

Fig. 7 shows the normalized $S-N$ curves, the maximum stress to respective ultimate strength for exposure environment, with experimental data in three environments. The closeness of the $S-N$ curves shown in Fig. 7 suggests that a single normalized $S-N$ curve can be used to predict the fatigue life of the investigated vinyl ester/E-glass fiber composite exposed to air, freshwater, or saltwater.

To determine the m value, (11) is rewritten into a simple linear form ($y = a + bx$)

$$\begin{aligned} \log(S_{\max}) &= -\frac{1}{2m} \log((n+1)C(1-R)^m) - \frac{1}{2m} \log N_f \\ &= \frac{1}{2m} \log \frac{1}{(n+1)C(1-R)^m} - \frac{1}{2m} \log N_f \end{aligned} \quad (19)$$

where

$$\begin{aligned} a &= \frac{1}{2m} \log \frac{1}{(n+1)C(1-R)^m} \\ b &= -\frac{1}{2m} \end{aligned}$$

Values of a and b are obtained from separate fatigue experimental data at 10 Hz in dry air, freshwater, and saltwater environments; and $m = -1/2b$. Table 2 represents these values and their standard errors for the three environments.

The small differences among the a and b values in the three environments confirm that a single normalized $S-N$ curve can be used to predict the fatigue life in these three environments. Fig. 8 shows the single linear regression that combines all

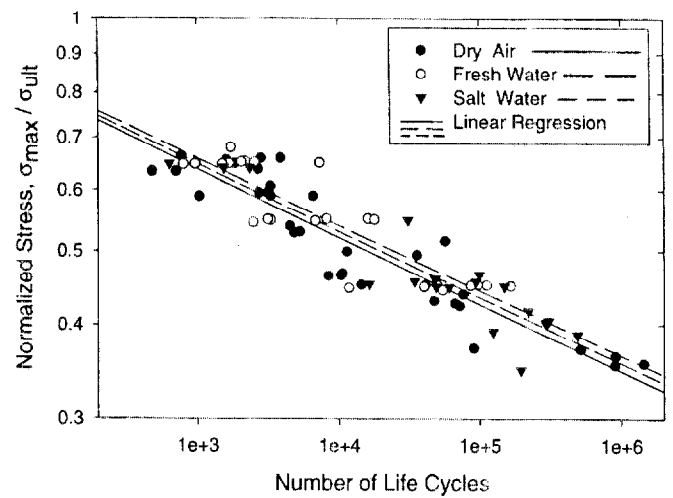


FIG. 7. Closeness of Normalized $S-N$ Curves in Three Environments

TABLE 2. Linear Constants and m Values for Three Environments

Environment (1)	a (22)	Standard error (3)	b (4)	Standard error (5)	m (6)	Standard error (7)
Dry air	0.0701	0.0272	-0.0882	0.0065	5.67	0.42
Freshwater	0.0766	0.0340	-0.0859	0.0085	5.82	0.53
Saltwater	0.0729	0.0450	-0.0869	0.0095	5.75	0.64
Three combined	0.0756	0.0181	-0.0877	0.0042	5.70	0.23

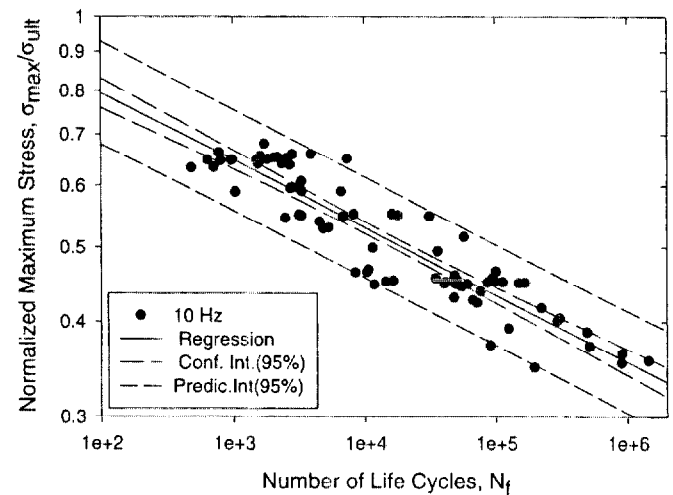


FIG. 8. $S-N$ Curve for Fatigue at 10 Hz in Three Environments

experimental data in the three environments. Besides the regression line, it also shows the 95% confidence interval and the 95% prediction interval. Overlapping Fig. 7 on Fig. 8, the three $S-N$ curves for three environments lie well within the 95% confidence interval. Thus, the error induced by a single normalized $S-N$ curve is well within the measurement uncertainty. Therefore, a single $S-N$ curve described by (8) can be used to predict the fatigue life of the investigated vinyl ester/E-glass fiber composite exposed to air, freshwater, or saltwater. The corresponding combined values of a , b , m , and their standard errors are also shown in Table 2.

When a and b values are substituted into (19), the $S-N$ curve for a vinyl ester/E-glass composite at 10 Hz and $N_f \geq 10$ may be expressed

$$(\sigma_{\max})^{11.40} N_f = 7.28 \quad (20)$$

for the three environments combined.

The value of n is determined from the partial damage data at different numbers of loading cycles under a given maximum load. An illustration of such data is displayed in Fig. 9 for 2 and 10 Hz. This figure shows that whenever substantial damage occurs, the curves become parallel. In other words, when the damage becomes substantial, it increases at a constant slope. Because we only measure the partial damage at the beginning of each order of magnitude (i.e., 10^3 , 10^4 , 10^5 , and 10^6), we may not accurately catch the number of cycles where the substantial damage starts. Fig. 9 also suggests that the damage growth within an order of magnitude of loading cycles ($dD/d \log N$) is constant and equals approximately 0.12. Therefore, for a given maximum applied load with two partial damages D_1 and D_2 measured at two respective numbers of loading cycles N_1 and N_2 , we have

$$\frac{N_2}{N_1} = 10$$

$$\frac{dD}{d \log N} = \frac{D_2 - D_1}{\log(N_2) - \log(N_1)} = \frac{D_2 - D_1}{\log \frac{N_2}{N_1}} = D_2 - D_1 = 0.12$$

From Fig. 10, D_1 starts from approximately 1–5%. Therefore,

$$\frac{D_2}{D_1} = \frac{D_1 + 0.12}{D_1} = 1 + \frac{0.12}{D_1} = 1 + (2.4-12)$$

Consequently, from (16) we may have

$$K_{12} = \frac{N_1 D_2}{N_2 D_1} = 0.34-1.3$$

However, from (6) and Fig 4, n must be ≥ 1

$$n = \frac{2(1 - K_{12})}{(D_1 - D_2 K_{12})} \geq 1 \quad (21a)$$

$$K_{12} \geq \frac{2 - D_1}{2 - D_2} = \frac{2 - D_1}{2 - 0.12 - D_1} \approx 1.065 \quad (21b)$$

$$1.065 \leq K_{12} \leq 1.3 \quad (21c)$$

$$n = \frac{2(K_{12} - 1)}{(D_2 K_{12} - D_1)} \approx \frac{2(K_{12} - 1)}{K_{12}(D_2 - D_1)} = \frac{2(K_{12} - 1)}{K_{12} \cdot 0.12} \quad (21d)$$

Thus we have

$$1.02 \leq n \leq 3.85$$

More experiments are required to determine the precise value of n . However, based on our limited experimental data and the function curves for $1/(1 - D)^n$ in Fig. 4, the smaller n value better represents the rapid growth of damage near the end of the life cycle. Therefore, the n value should be closer to the lower bound. For now, we suggest $n = 2$.

The parallel damage slopes in Fig. 9 for 2 and 10 Hz suggest that, for the composite used in this study, n does not appear to be sensitive to frequency. If the composite is sensitive to frequency, it must lie in the C coefficient. Previous studies reported that the modulus and strength of composite materials are higher at high frequency than that at low frequency (Sun and Chan 1979; Mandell and Meier 1983; Dlubac et al. 1990; Weissman and Chartoff 1990). If we assume that composites fatigued at a lower frequency fail at a lower number of cycles for a given maximum applied load, then the C constant will be higher at a lower frequency. The relationship between fatigue damage and frequency has been proposed by Wnuk (1974b) for other solid materials. His model has the form

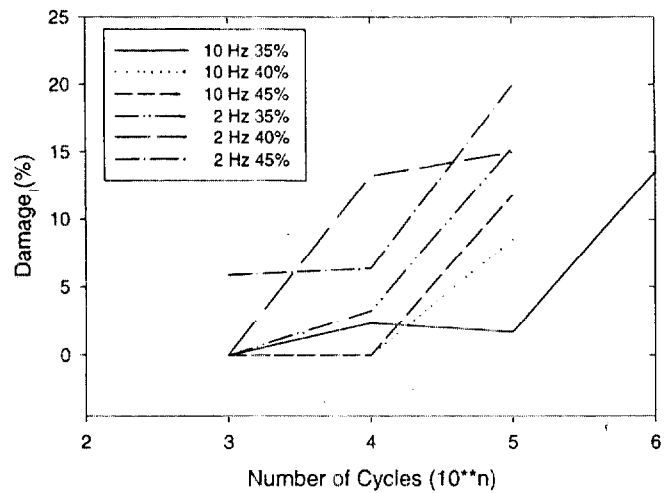


FIG. 9. Partial Damage at Selected Loading Cycles

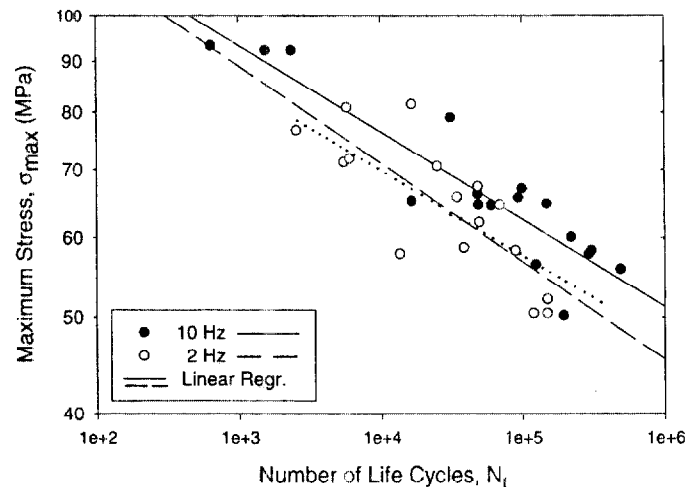


FIG. 10. Fatigue at 2 and 10 Hz in Saltwater

$$\frac{da}{dN} = \lambda_1 \left(\frac{\Delta K}{K_{IC}} \right)^m + \frac{\lambda_2}{f} \left(\frac{\Delta K}{K_{IC}} \right)^n \quad (22)$$

where K_{IC} = stress intensity for mode I fracture; ΔK = stress intensity amplitude; λ_1 and λ_2 = constants; and f = frequency.

In this study, C as a function of frequency may be written

$$C = C_1 + \frac{C_2}{f} \quad (23)$$

where C_1 and C_2 = constants; and f = frequency.

Substituting C into (7) and (8), we obtain

$$\frac{1}{n+1} - \frac{(1-D)^{n+1}}{n+1} = \left(C_1 + \frac{C_2}{f} \right) (S_{\max}^2(1-R))^m N \quad (24)$$

$$\frac{1}{n+1} = \left(C_1 + \frac{C_2}{f} \right) (S_{\max}^2(1-R))^m N_f \quad (25)$$

To determine the C_1 and C_2 , we rely on experimental data at two frequencies. Fig. 10 displays the linear-fit $S-N$ lines for the saltwater environment at 2 and 10 Hz frequencies. The $S-N$ line for 2 Hz is below that for 10 Hz. From this figure, it appears that for a given maximum applied load, the number of cycles at failure for 2 Hz is less than that for 10 Hz. The small difference between the slopes and the $S-N$ curves for 2 and 10 Hz could be due to inability to statistically average out experimental variations by the limited number of samples. The scattering of the experimental data from the $S-N$ curve for 2

Hz is obviously greater than that for 10 Hz. If we reconstruct the $S-N$ curve for 2 Hz using the same slope of the $S-N$ curve for 10 Hz as shown in the dotted line, the newly constructed $S-N$ curve also reasonably fits the experimental data for 2 Hz. Therefore, we can state that neither the slope of the $S-N$ curve for vinyl ester/E-glass fiber nor the m value appears to be sensitive to frequency.

By taking a logarithm on both sides of (25) and substituting the σ_{\max} and N_f for 2 and 10 Hz, respectively, into the equation, two separate equations for respective 2 and 10 Hz can then be subtracted from each other. These two parallel $S-N$ curves relate the C_2/f to C_1

$$\log \left(C_1 + \frac{C_2}{2} \right) - \log \left(C_1 + \frac{C_2}{10} \right) = 2m(\log \sigma_{\max,10} - \log \sigma_{\max,2}) = 0.445$$

where $\sigma_{\max,10}$ and $\sigma_{\max,2}$ = the maximum stresses for 10 and 2 Hz, respectively

$$\frac{C_1 + \frac{C_2}{2}}{C_1 + \frac{C_2}{10}} = 2.78$$

$$\frac{C_2}{C_1} = 8$$

Eqs. (24) and (25) can then be rewritten

$$\frac{1}{n+1} - \frac{(1-D)^{n+1}}{n+1} = C_1 \left(1 + \frac{8}{f} \right) (S_{\max}^2(1-R))^m N \quad (26)$$

$$\frac{1}{n+1} = C_1 \left(1 + \frac{8}{f} \right) (S_{\max}^2(1-R))^m N_f \quad (27)$$

As for partial damage, Fig. 3 shows that the residual modulus is higher at 10 Hz than at 2 Hz, which is consistent with several previous studies (Sun and Chan 1979; Mandell and Meier 1983; Dlubac et al. 1990; Weissman and Chartoff 1990).

It should be emphasized that experimental data generated from the composite used in this study is in good agreement with the proposed model. The validation of this model for polymeric composites made with other matrices and fibers is being investigated.

SUMMARY AND CONCLUSIONS

A fatigue model based on the cumulative damage due to cyclic loading is developed and verified with experimental data for a vinyl ester/E-glass polymer composite. The fatigue damage per cyclic loading, residual modulus in terms of partial damage, and fatigue life of fiber-reinforced composites are described as functions of applied maximum stress, stress amplitude, loading frequency, state of damage, and material constants as follows:

$$\frac{dD}{dN} = \left(C_1 + \frac{C_2}{f} \right) \frac{(S_{\max}^2(1-R))^m}{(1-D)^n} \quad (28)$$

$$\frac{1}{n+1} - \frac{(1-D)^{n+1}}{n+1} = \left(C_1 + \frac{C_2}{f} \right) (S_{\max}^2(1-R))^m N \quad (29)$$

$$\frac{1}{n+1} = \left(C_1 + \frac{C_2}{f} \right) (S_{\max}^2(1-R))^m N_f \quad (30)$$

The material constants used in the model are determined using the experimental data. This model can be used to predict the fatigue life of a vinyl ester/E-glass polymer composite at an applied load and to predict the residual strength modulus after a number of cycles at a given load in various civil en-

gineering and offshore environments. Using the experimental data to determine the model constants, we have obtained the following $S-N$ curve for a glass fiber reinforced vinyl ester composite exposed to the three environments

$$S_{\max}^{11.40} N_f = \frac{13.11}{1 + \frac{8}{f}} \quad (31)$$

for the three environments combined; where S_{\max} = normalized stress to respective static ultimate strength ($|S_{\max}| \leq 1$).

The residual modulus for a given maximum applied load after N loading cycles may be predicted

$$\frac{E}{E_0} = \left(1 - \frac{S_{\max}^{11.40} N \left(1 + \frac{8}{f} \right)^{1/(n+1)}}{13.11} \right)^n \quad (32)$$

for the three environments combined. The value of n is not conclusive at this time; more experiments are required to determine its precise value. Our experiment data indicate that n should lie between 1.02 and 3.85. However, Fig. 4 shows that the smaller n value better represents the rapid growth of damage near the end of the life cycle. For now, we suggest $n = 2$.

The vinyl ester/E-glass fiber composite loses about 25 and 30% of its tensile strength in freshwater and saltwater, and 15% and 11% of tensile modulus, respectively. For the material used in this study, the loss in tensile strength and modulus in saltwater is approximately the same as that in freshwater, and the fatigue life of the composite in these aqueous environments is shorter than that in air.

ACKNOWLEDGMENT

The writers gratefully appreciate the support of the NIST Advanced Technology Program, Gaithersburg, Md.

APPENDIX. REFERENCES

- Adimi, R., Rahman, H., Benmokrane, B., and Kobayashi K. (1998). "Effect of temperature and loading frequency on the fatigue life of a CFRP bar in concrete." *Fiber Compos. in Infrastructure, Proc., 2nd Int. Conf. on Compos. in Infrastructure*, H. Saadatmanesh and M. R. Ehsani, eds., Univ. of Arizona, Tucson.
- Ashbee, K. (1993). *Fundamental principles of fiber reinforced composites*. Technomic Publishing Co., Lancaster, Pa.
- Bevington, P. R., and Robinson, D. K. (1992). *Data reduction and error analysis for the physical sciences*. McGraw-Hill, New York.
- Chiou, P., and Bradley, W. L. (1996). "Moisture-induced degradation of glass/epoxy filament-wound composite tubes." *J. Thermoplastic Compos. Mat.*, 9, 118-128.
- Dlubac, J. J., Lee, G. F., Duffy, J. V., Deigan, R. J., and Lee, J. D. (1990). "Comparison of the complex dynamic modulus as measured by three apparatus." Chapter 3, *Sound and vibration damping with polymers*, ACS Symposium Series 424, R. C. Corsaro and L. H. Sperling, eds., Am. Chem. Soc., Washington, D.C., 49-62.
- Hofer, K. E., Skaper, G. N., Bennett, L. C., and Rao, N. (1987). "Effect of moisture on fatigue and residual strength losses for various composites." *J. Reinforced Plastics and Composites*, 6, 53-65.
- Garrels, R. M., and Thompson, M. E. (1962). "A chemical model for sea water." *Am. J. Sci.*, 260, 57-62.
- Jang, B. Z. (1994). *Advanced polymer composites: Principles and applications*. ASM International, Materials Park, Ohio.
- Kadi, H., and Ellyin, F. (1994). "Effect of stress ratio on the fatigue of unidirectional glass fibre/epoxy composite laminae." *Compos.*, 25(10), 917-924.
- Komai, L., Minoshima, K., and Shiroshita, S. (1991). "Hygrothermal degradation and fracture process of advanced fibre-reinforced plastics." *Mat. Sci. & Eng.*, A143, 155-166.
- Liu, B., and Lessaed, L. B. (1994). "Fatigue and damage-tolerance analysis of composite laminates: Stiffness loss, damage-modeling, and life prediction." *Compos. Sci. and Technol.*, 51, 43-51.
- Mandell, J. (1982). "Fatigue behavior of fibre-resin composites." Chapter 4, *Developments in reinforced plastics*, G. Pritchard, ed., Applied Science Publishers, London, 67-107.

- Mandell, J., and Meier, U. (1983). *Effects of stress ratio, frequency, and loading time on the tensile fatigue of glass-reinforced epoxy*, ASTM STP 813, T. K. O'Brien, ed., ASTM, West Conshohocken, Pa.
- Martin, R., ed. (1995). *Composite materials: Fatigue and fracture*, ASTM STP 1230, ASTM, West Conshohocken, Pa.
- Ogin, S. L., Smith, P. A., and Beaumont, W. R. (1985). "Matrix cracking and stiffness reduction during the fatigue of a (0/90) GFRP laminate." *Compos. Sci. and Technol.*, 23, 23–31.
- Plumtree, A., and Shen, G. (1991). "Fatigue damage evolution and life prediction." *Proc., 8th Int. Conf. on Compos. Mat.*, 4, 38M/1–38M/10.
- Reifsnider, K. L., ed. (1979). *Damage in composites*, ASTM STP 775, ASTM, West Conshohocken, Pa.,
- Reifsnider, K. L., ed. (1991). *Fatigue of composite materials, composite materials series*. Vol. 4, Elsevier Science, Amsterdam.
- Reifsnider, K. L. (1994). "Micromechanical modeling of polymeric composites." *Polymer*, 35, 5035–5040.
- Saadatmanesh, H., and Ehsani, M. R., eds. (1998). "Fiber composites in infrastructure." *Proc., 2nd Int. Conf. on Compos. in Infrastructure*, Univ. of Arizona, Tucson.
- Spearing, S. M., Beaumont, P. W. R., and Ashby, M. F. (1992). "Fatigue damage mechanics of composite materials: II—A damage growth model." *Compos. Sci. and Technol.*, 44, 169–177.
- Springer, G. S., Sanders, B. A., and Tung, R. W. (1980). "Environmental effects on glass fiber reinforced polyester and vinylester composites." *J. Compos. Mat.*, 14, 213–232.
- Subramanian, S., Reifsnider, K. L., and Stinchcomb, W. W. (1995). "A cumulative damage model to predict the fatigue life of composite laminates including the effect of a fiber-matrix interphase." *Int. J. Fatigue*, 17(5), 343–351.
- Sun, C. T., and Chan, W. S. (1979). "Frequency effect on the fatigue life of a laminated composite." *Compos. Mat., Testing and Design*, ASTM STP 674, S. W. Tsai, ed., ASTM, West Conshohocken, Pa., 418–430.
- Thionnet, A., and Renard, J. (1994). "Laminated composites under fatigue loading: A damage development law for transverse cracking." *Compos. Sci. and Technol.*, 52, 173–181.
- Talreja, R. (1987). *Fatigue of composite materials*. Technomic Publishing Co., Lancaster, Pa.
- Wang, S. S., and Fitting, D. W., eds. (1995). "Composites materials for offshore operations." *Proc., 1st Int. Workshop, Nat. Inst. of Standards and Technol., Spec. Publ. 887*, Gaithersburg, Md.
- Watanabe, M. (1979). "Effect of water environment on fatigue behavior of fiberglass reinforced plastics." *Proc., 5th Conf. Compos. Mat.: Testing and Design*, ASTM STP 674, S. W. Tsai, ed., ASTM, West Conshohocken, Pa., 345–367.
- Weissman, P. T., and Chartoff, R. P. (1990). "Extrapolating viscoelastic data in the temperature-frequency domain." Chapter 7, *Sound and vibration damping with polymers*, ASC Symposium Series 424, R. C. Corsaro and L. H. Sperling, eds., Am. Chem. Soc., Washington, D.C., 111–131.
- Wnuk, M. P. (1974a). "Subcritical growth of fracture (inelastic fracture)." *Int. J. Fracture Mech.*, 7, 383–407.
- Wnuk, M. P. (1974b). "Fatigue in rate sensitive solids." *Int. J. Fracture Mech.*, 10, 223–226.
- Ye, L. (1989). "On fatigue damage accumulation and material degradation in composite materials." *Compos. Sci. and Technol.*, 36, 339–350.